ACS APPLIED MATERIALS & INTERFACES

www.acsami.org

Research Article

Selective Adsorption and Efficient Degradation of Petroleum Hydrocarbons by a Hydrophobic/Lipophilic Biomass Porous Foam Loaded with Microbials

Lihua Chen,* Kaihui Xu, Yuhan Zhang, Qimeige Hasi, Xiaofang Luo, Juanjuan Xu, and An Li*

Cite This: *ACS Appl. Mater. Interfaces* 2021, 13, 53586–53598

Read Online

ACCESS | Metrics & More | Article Recommendations | Supporting Information

ABSTRACT: Highly efficient elimination of petroleum pollution is of great importance for addressing environmental issues and social sustainability. In this study, we demonstrate a novel strategy for efficient elimination of petroleum pollution by selective adsorption of it by an ultralight hydrophobic/lipophilic microorganism-loaded biomass porous foam (BTS-MSFT4@MTMS) followed by a green degradation of adsorbates under mild conditions. The porous structure of biomass porous foam (MSFT) could provide plenty of room for immobilization of *Bacillus thuringiensis* (BTS), while a simple surface modification of the MSFT load with a BTS strain (BTS-MSFT4) by methyltrimethoxysilane (MTMS) could change its wettability from hydrophilic to lipophilic, which makes selective adsorption of hydophobic petroleum pollution from water for biodegradation possible. As expected, using a petroleum *n*-hexadecane solution with a concentration of 3% as a model oily wastewater, the as-prepared BTS-MSFT4@MTMS possesses both a superior selective adsorption of ca. 99% and high degradation activity with a high degradation rate of up to 86.65% within 8 days under the conditions of 37 °C, 120 r min^{-1}, and pH = 7, while the degradation rates for the BTS-MSFT4 and the free BTS strain were measured to be only 81.62 and 65.65%, respectively, under the same conditions. In addition, the results obtained from the study on environment tolerance show that the BTS-MSFT4@MTMS exhibits a strong tolerance under different conditions with various pHs, temperatures, and initial concentrations. Compared with the existing methods for removal of petroleum pollution by direct adsorption of petroleum pollution via superoleophilic porous materials or applying free microorganisms for biodegradation only, which suffers the drawbacks of low selectivity or poor efficiency, our method has great advantages of cost-effectiveness, scalable fabrication, and high efficiency without secondary pollution. Moreover, such a two-in-one strategy by integration of both selective adsorption and biodegradation into biodegradable BTS-MSFT4@MTMS may particularly have great potential for practical application in environmental remediation.

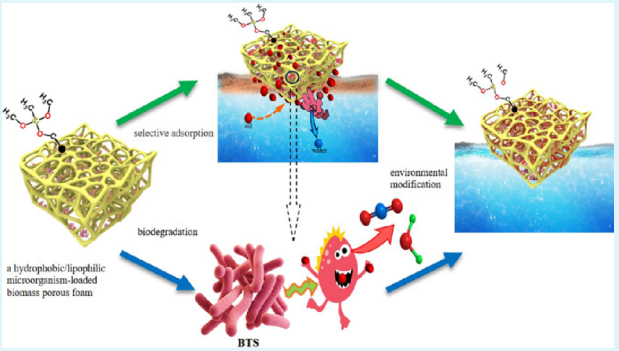

KEYWORDS: *Bacillus thuringiensis, microbial remediation, hyperwetting, methyltrimethoxysilane, preferential adsorption*

1. INTRODUCTION

With the rapid development of modern industry, agriculture, and urbanization, the increasingly serious environmental pollution has caused a serious impact on the sustainable development of the human society. Petroleum is one of the most important sources of fuel and the energy resource basis of modern petrochemical industry worldwide.[1−3] However, the exploitation, transportation, storage, and use of petroleum would inevitably generate a large amount of petroleum hydrocarbon pollutants in soil and water.[4−6] In particular, as one of the most common petroleum pollutants, polycyclic aromatic hydrocarbons and hydrocarbon pollutants have aroused more and more attention owing to their high environmental toxicity and biological accumulation.[7−9] Therefore, there is an urgent need to exploit efficient and green technologies or functional materials to address the serious environmental issues caused by petroleum pollutants.[10]

At present, three kinds of main technologies, i.e., physical, chemical, and biological methods, have been successfully applied for treatment of oily wastewater.[11−14] The chemical method has obvious limitations for its inevitable involvement of the use of chemicals, which may pose a risk for secondary environmental pollution.[15−18] Comparatively, the physical adsorption method is more favorable owing to its simple operation and fast treatment effects. In particular, the recent progress in this direction by creation and employment of

Received: August 12, 2021
Accepted: October 26, 2021
Published: November 5, 2021

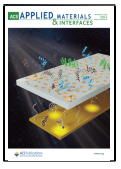

https://doi.org/10.1021/acsami.1c15380
ACS Appl. Mater. Interfaces 2021, 13, 53586−53598

superwetting materials, e.g., superhydrophobic or superoleophilic porous materials or membranes,[19] shows great potential for treatment of oily wastewater on the basis of the unique surface wettability of these materials, which makes selective adsorption of petroleum (or organic pollutants) without adsorption of water possible, thus resulting in high efficiency for removal of the organic contaminants.[20−22] Unfortunately, however, a great challenge still remains as the complicated or expensive fabrication process for these superwetting materials in most of the cases would dramatically impair their practicability and in turn hinder their application on a large scale. On the other hand, the disposal of these superwetting materials after use still poses a risk for secondary environmental pollution.[23−25]

Compared with these two technologies mentioned above, the biological method has the advantages of cost-effectiveness, simple operation, environment-friendliness, and, importantly, no secondary pollution.[26−29] Among them, immobilized microorganism technology is one of the most important and efficient biological methods for biodegradation of petroleum pollutants. For immobilized microorganism technology, the immobilization of the microorganisms in a certain carrier material usually with a porous structure and a large accessible area by using adsorption/embedding methods is essential.[30−32] At the same time, the immobilized microorganisms can normally grow up and densely distribute in the surface of the carrier materials, by using petroleum hydrocarbons as a carbon and energy source to maintain their own metabolism and biological activity.[33−36] In this way, the petroleum pollutants could be therefore biodegraded and eliminated; microorganisms have been rapidly developed and widely used as one of the effective ways for removal of petroleum hydrocarbon pollutants.[37−39] Although great progress has been made in this field, there are still great challenges connected with less immobilization amounts, low activity, or weak immobilization strength of microorganisms to porous substrates, e.g., activated carbon. In addition, the usually hydrophilic nature of carrier materials leads to their poor affinity to hydrophobic pollutants, resulting in a low adsorption selectivity, low degradation rate, and prolonged degradation time in terms of an acceptable degradation standard.

In this study, we demonstrate, for the first time, a new strategy for selective adsorption and then efficient biodegradation of petroleum pollutants by fabrication and employment of an ultralight and lipophilic microorganism-loaded biomass porous foam under mild conditions. The porous structure of biomass porous foam (MSFT) could provide plenty of room for immobilization of much more BTS strains, while a simple surface modification of the MSFT by MTMS could change its wettability from hydrophilic to hydrophobic, which makes selective adsorption of hydrophobic petroleum pollution from water for biodegradation possible. Particularly, the biomass nature of the MSFT could provide a carbon source for maintaining the microorganisms' own metabolism and biological activity. Under our conditions, the as-resulted foam possesses a high adsorption selectivity, superior degradation rate, and desired environmental tolerance. By the combination of its abundant resource, cost-effectiveness, and scalable manufacture, such a BTS strain-loaded superwetting biomass porous foam may have great potential for practical applications in petroleum or organic industrial pollutant elimination.

2. EXPERIMENTAL SECTION

2.1. Materials. *n*-Hexadecane ($C_{16}H_{34}$) was purchased from Shanghai Macklin Biochemical Co., Ltd. Epoxy resin ($(C_{11}H_{12}O_3)_n$) was purchased from Jinan Yunbaihui Biotechnology Co., Ltd. A nutrient broth medium (dry powder) and a nutrient agar medium (dry powder) were purchased from Hangzhou Microorganism Reagent Co., Ltd. Sodium hypochlorite ($NaClO_2$), acetic acid (CH_3COOH), ethanol (C_2H_5OH), and calcium nitrate ($Ca(NO_3)_2$) were all purchased from the Tianjin Guangfu Chemical Reagent Factory, polyvinyl alcohol ($(C_2H_4O)_n$) was purchased from Shanghai Aladdin Biochemical Technology Co., Ltd., methyltrimethoxysilane ($CH_3Si(CH_3O)_3$) was purchased from Chengdu Aikeda Chemical Reagent Co., Ltd., and *n*-hexane (C_6H_{14}) was purchased from Shanghai Aladdin Biochemical Technology Co., Ltd. Among them, cetane and *n*-hexane were of chromatographic purity, and other chemical reagents and solvents were analytical reagents, which can be used directly without further purification.

2.2. Culture of the BTS Strain Suspension. The BTS microorganism inoculum was a strain that was screened by a research group to degrade petroleum hydrocarbons efficiently.[40] We used about 100 μL of activated BTS and inoculated it in a sterile nutrient broth medium and cultured it with shaking at 37 °C and 120 r min^{-1}. After 48 h, turbidity was observed, and the number of colonies reached more than 1×10^8 cfu mL^{-1}; they were taken out and stored in a refrigerator at 4 °C.

2.3. Preparation of the Ultralight and Hydrophilic Sunflower Receptacle. A dried sunflower receptacle (named as SFT) was cut into 2 × 2.5 cm and put into a beaker. $NaClO_2$ solution (250 mL, 1%) and 0.5 mL of CH_3COOH were added and stirred at 75 °C for 2 h. Then, we added 2.5 g of $NaClO_2$ and 0.5 mL of CH_3COOH to the above reaction solution, and this step was repeated 4 times. After the reaction was finished, the solution was cooled to room temperature, and the pH was adjusted to neutral. Finally, the ultralight hydrophobic sunflower receptacle material named MSFT was obtained by freeze-drying for 48 h.

2.4. Immobilization of the BTS Strain. The MSFT was sterilized by high-pressure steam at 121 °C for 30 min and cooled to room temperature. First, the MSFT was immersed in PVA solution of 3% mass concentration until it was completely wet, removing excess PVA by suction filtration and washing its surface with distilled water to prevent blockage of the outer wall channel. Second, the quantitative microorganism suspension was added to the MSFT, and it was left for about 30 min until it was completely absorbed. Third, the porous material with the immobilized BTS strain suspension was dried at 37−40 °C for 2 h, which was beneficial for the microorganism agent to be concentrated and loaded on the PVA surface or be wrapped in it. Then, a $Ca(NO_3)_2{\cdot}4H_2O$ solution of 5% concentration (20 mL) was added and reacted for 30 min at 4 °C. Lastly, the excess $Ca(NO_3)_2{\cdot}4H_2O$ solution was filtered, and this process was repeated 4 times. The carriers after the first, third, fourth, and fifth immobilization of the BTS strain suspension were named BTS-MSFT1, BTS-MSFT3, BTS-MSFT4, and BTS-MSFT5, respectively.

2.5. Hydrophobic and Lipophilic Surface Remodification after Immobilization of the BTS Strain. We added acetone (10 mL) into a beaker containing epoxy resin (16 g), stirred it fully, and dissolved it, MTMS (10 mL) was added to 8 g of the mixed solution, and finally, the mixed modified solution was sprayed on the surface of the BTS-MSFT4. The obtained hydrophobic and lipophilic modified material was named BTS-MSFT4@MTMS.

2.6. Characterization. Gas chromatography (GC) (Clarus GC-TotalChrom, PerkinElmer Instruments (Shanghai) Co., Ltd.) was used for quantitative analysis; the column temperature was 180 °C, which was maintained for 2 min; the temperature of the injector and the FID detector was 220 °C; the fixed flow rates of nitrogen, hydrogen, and air were 20, 45, and 450 mL min^{-1}, respectively. Gas chromatography−mass spectrometry (GC−MS) (thermo GC−MS DSQII) was used for qualitative analysis; the test conditions were similar to GC. A scanning electron microscope (SEM) (JSM-6700F) was used to characterize the material morphology. The pore size and porosity of samples were measured by mercury injection (Auto Pore

https://doi.org/10.1021/acsami.1c15380
ACS Appl. Mater. Interfaces 2021, 13, 53586−53598

IV-9500). Images of superhydrophilic or ultralight petroleum were recorded by a high-speed video camera system. An energy-dispersive spectrometer (EDS) (Octane SDD) was used to observe the elemental distribution of the material. X-ray diffraction (XRD) of the material was performed on a Rigaku Geigerflex D/max series instrument. Fourier transform infrared spectroscopy (FTIR) (Nicolet 380, US) was used to study the functional groups of the material. X-ray photoelectron spectroscopy (XPS) (PHI 5702, US) was used to study the elemental composition and the molecular structure of the material. In addition, the contact angle was used to characterize the wettability. The mechanical properties of materials were tested by a universal testing machine (SHIMADZU AGS-X). An ultraviolet spectrophotometer (MAPADA P2PC) was used to test the absorbance of diesel oil and gasoline.

2.7. Simulated Petroleum *n*-Hexadecane Degradation Experiments. In this study, *n*-hexadecane was used as simulated petroleum for degradation experiments. The experiment was divided into four groups, including experimental group I (namely, BTS-MSFT4), experimental group II (namely, BTS-MSFT4@MTMS), the control group (namely, the free BTS agent), and the blank group (namely, MSFT). First, the degradation activities of experimental groups I and II and control and blank groups on the simulated petroleum *n*-hexadecane of 3% concentration (relative to the adsorption capacity of the microorganism liquid) were determined at different times such as 12, 24, 72, 120, and 192 h and investigated under the conditions of 37 °C, 120 r min^{-1}, and pH 7. Then, the tolerance of BTS-MSFT4@MTMS for the environment was explored under the conditions of different initial concentrations, temperatures, and pHs. The times of recycling and tolerance of BTS-MSFT4@MTMS were also discussed.

3. RESULTS AND DISCUSSION

As shown in Figure 1, at first, the sunflower receptacle (SFT) was pretreated by drying and cutting it into pieces for use. The

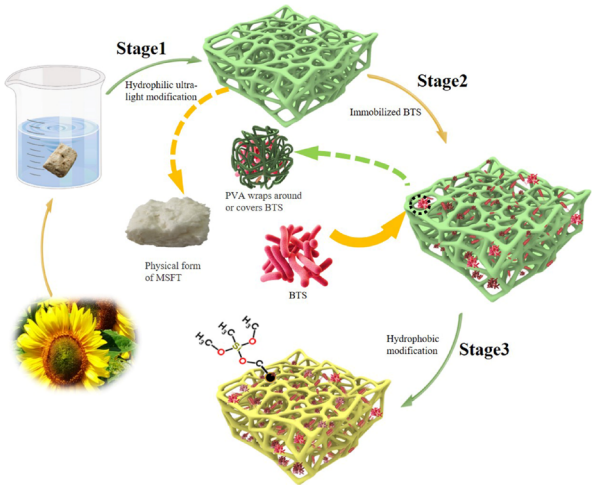

Figure 1. Schematic illustration of the preparation of the BTS-MSFT4@MTMS adsorption degradation agent.

SFT was modified into the hydrophilic porous material MSFT by hydrolysis to remove lignin (stage 1), then PVA was used as an adhesive, and the BTS strain was immobilized in the MSFT many times (stage 2). After loading the BTS strain, the surface of the BTS-MSFT was remodified with MTMS to achieve a surficial hydrophobic wettability for selective adsorption of oils or petroleum contaminants from water (stage 3). Finally, the absorbed oils or petroleum contaminants could be biodegraded by BTS microorganisms in a green pattern.

In order to observe the variety of the surface wettability of the SFT before and after modification, the measurement of the water contact angle (WCA) was carried out, and the results are shown in Figure 2a–d. The obvious changes in wettability of

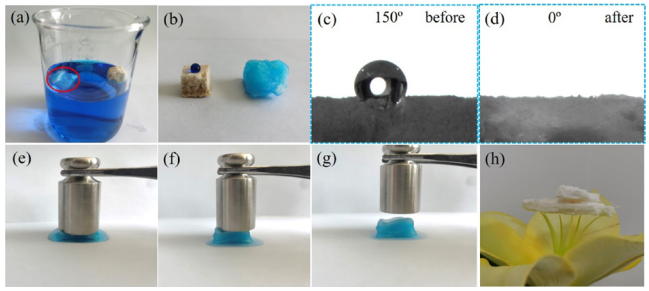

Figure 2. (a,b) Schematic diagrams of hydrophilicity of the MSFT, (c) WCA of the SFT and (d) MSFT, (e–g) shape changes of the MSFT under pressure to show its elasticity, and (h) photograph of the MSFT on a flower core of lily to show its ultralight property.

the SFT can be found: (1) The untreated SFT has a hydrophobic structure with a WCA of 150°. The water contact angle of the SFT changes from 150 to 0° after hydrophilic modification, that is, the hydrophobic SFT turns to be hydrophilic, which facilitates a high uptake for the BTS strain. (2) The modified SFT (abbreviated as MSFT) has sponge-like elasticity after absorbing water (as shown in Figure 2e–g), which is beneficial to the repeated concentration and immobilization of BTS in the later period. (3) The MSFT also has ultralight properties and can self-float on the surface of water, which would be advantageous to the practical operation and collection for elimination of organic pollutants (as shown in Figure 2h). From the shot images (Figure S1), it can be seen that the time from droplet dropping to complete immersion is less than 1 s, showing the superhydrophilicity of the MSFT, which provides the prerequisite for the subsequent immobilization of the BTS strain.

The X-ray diffraction pattern (XRD) of the MSFT is shown in Figure 3a, and the peak type indicates that the cellulose used in this work is natural cellulose I. I_{am} is the diffraction intensity at $2\theta = 18.3°$, and I_{002} is the diffraction intensity at $2\theta = 22.5°$. The crystallinity is 39% calculated using formula S1, indicating that the MSFT has strong elasticity, hygroscopicity, softness, and chemical reactivity. It is beneficial to the concentration of the immobilized BTS strain many times in the later stage.

The Fourier transform infrared spectra (FTIR) of the SFT and MSFT are shown in Figure 3b. The characteristic adsorption peak at 3422.84 cm^{-1} becomes much stronger, which is assigned to the hydrophilic group of O–H. The peak at 2925.97 cm^{-1} is attributed to the vibration of the C–H bond of methyl, and methylene groups also exhibited the same phenomenon. The stretching vibration peak of the MSFT and SFT near 1631.22 cm^{-1} indicates the existence of C=O groups, and the peak is enhanced after hydrophilic ultralight modification. In the MSFT, the stretching vibration peaks at 1397.80, 1249.21, and 1057.75 cm^{-1} belong to the functional groups $-CH_3$, C–O, and C–O–C, respectively, among which the C–O–C group is caused by the stretching vibration of the β (1→4)-acetyl group in the cellulose. Through the above analysis, it is clearly proven that the hydrophobic lignin of the SFT is removed and the hydrophilic and lipophilic cellulose is exposed. There are three peaks in the C 1s spectrum of X-ray photoelectron spectroscopy (XPS) (as shown in Figure 3c): 284.7, 286.2, and 287.8 eV belonging to C=C, C–O, and C=O bonds, respectively. The O 1s spectrum (as shown in Figure

https://doi.org/10.1021/acsami.1c15380
ACS Appl. Mater. Interfaces 2021, 13, 53586–53598

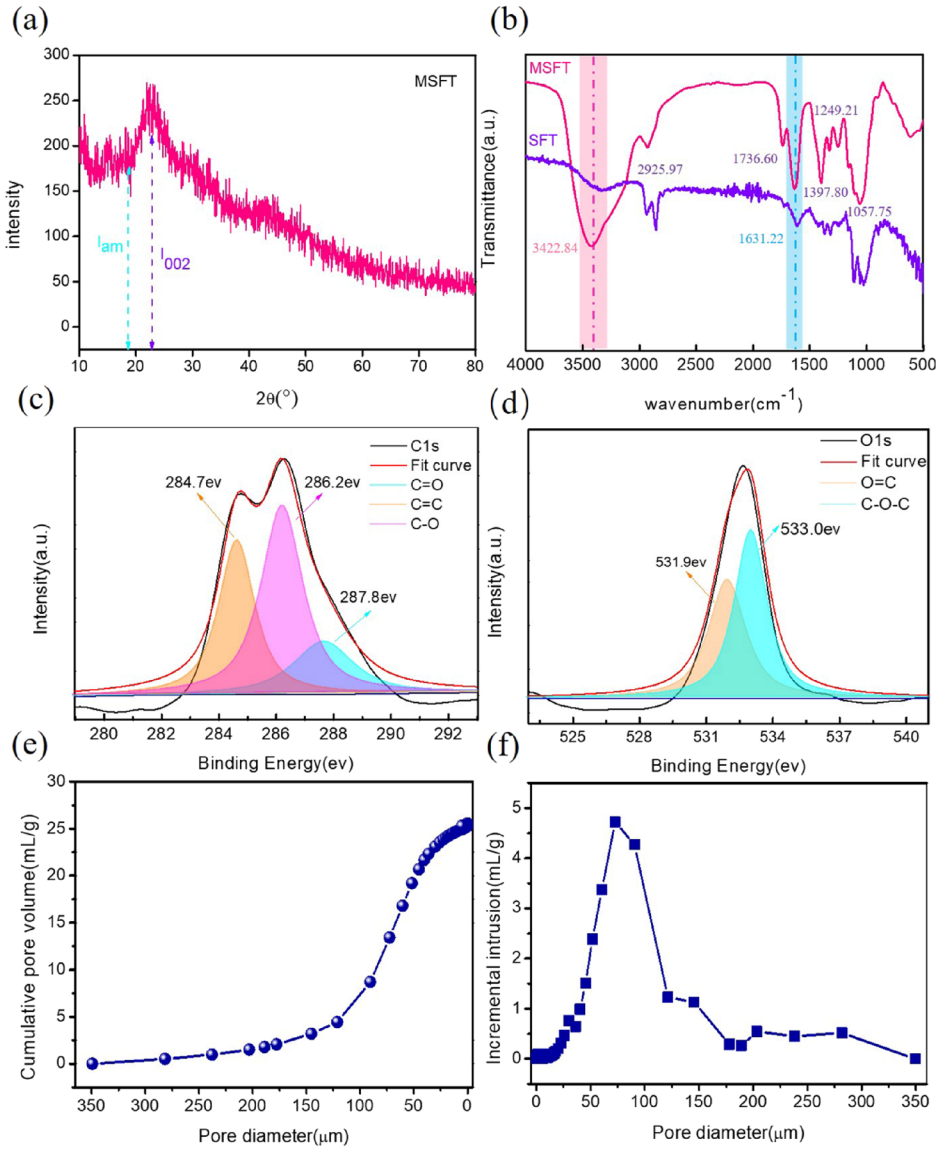

Figure 3. (a) XRD spectrum of the MSFT, (b) FTIR spectra of the MSFT and SFT, high-resolution XPS spectra for (c) O 1s and (d) C 1s of the MSFT, (e) mercury intrusion/extrusion curve, and (f) pore diameter distribution of the MSFT.

4d) contains two peaks at 531.9 and 533.0 eV, which are attributed to O═C and C−O−C, respectively. The above functional groups are consistent with those of the FTIR spectrum. It can be concluded that the MSFT has super-hydrophilic wettability and strong stability. The mercury porosimetry measurements demonstrate the macroporous structure of the carbon replicas (Figure 3e,f). From the mercury intrusion/extrusion curves, when the diameter is 350−120 μm, the pore volume amount increases slowly, and when the diameter is 120−0 μm, the pore volume amount increases rapidly. Moreover, the cumulative range of its pore size is 0−60 μm. The porosity is 92.99%, and the total pore area is 4.570 $m^2\ g^{-1}$. Both indicate that the MSFT has a macroporous structure.

The scanning electron microscope (SEM) images of the porous structure of the modified material MSFT and the quantitative and morphological changes after the MSFT immobilized BTS 1, 3, and 5 times are shown in Figure 4. The results indicate that the MSFT possesses a porous network structure (Figure 4a), which provides plenty of room for increasing the number of immobilized microorganisms and promoting good growth of microbes inside, thus improving the degradation efficiency. The microorganism agent BTS used in the study was elliptical or rod-shaped (as shown in Figure 4b). As shown in Figure 4c, the density distribution of the microorganism agent fixed onto the MSFT by direct one-time adsorption is small; however, the distribution of BTS strain agents in the MSFT with PVA as an adhesive becomes more intensive with the increase in the number of fixation times (1 time (Figure 4d), 3 times (Figure 4e), and 5 times (Figure 4f)) and is also much higher than that by direct one-time adsorption (Figure 4b). As shown in Figure 4g, the quantity of immobilized BTS increases with the increase in the number of immobilization and gradually tends to be saturated at 4 times (abbreviated as BTS-MSFT4, used as a model for the following test), which is also consistent with the SEM results.

The BTS strain of BTS-MSFT4 was diluted to 10^{-8} by the method of crushing and soaking, and the number of live bacteria was calculated to be 1.15×10^{11} cfu mL^{-1} (as shown in Figure S2 and the inset of Figure 4g), which was 1000 times

https://doi.org/10.1021/acsami.1c15380
ACS Appl. Mater. Interfaces 2021, 13, 53586−53598

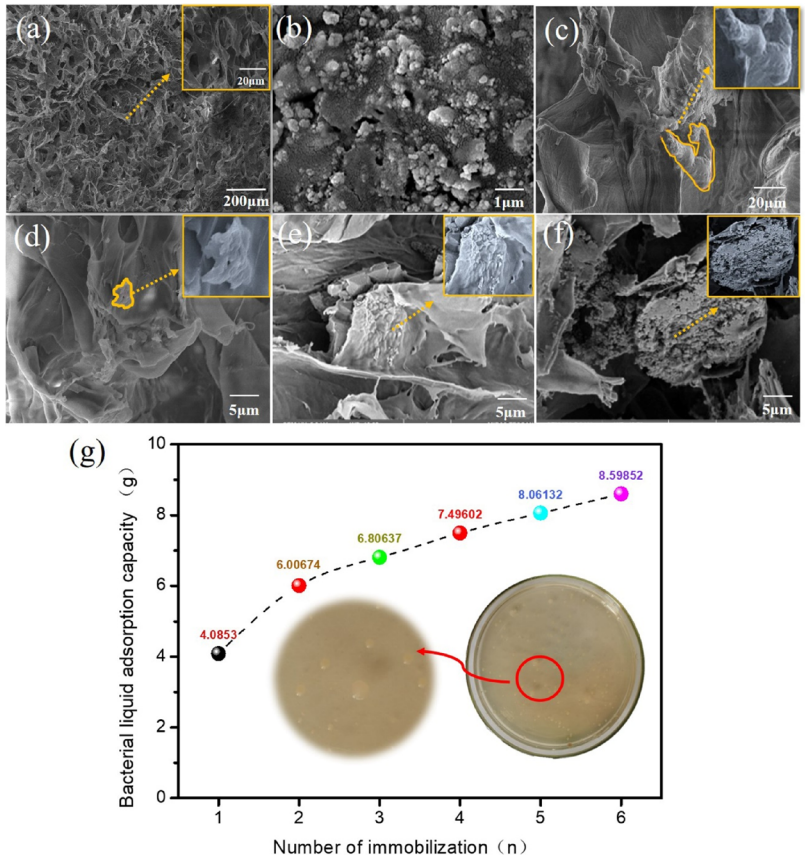

Figure 4. (a) SEM images of the MSFT; (b) morphology of the BTS strain; (c) SEM images of the MSFT material fixed with the BTS microorganism inoculum once; (d–f) SEM images of BTS-MSFT1, BTS-MSFT3, and BTS-MSFT5; (g) quantitative diagram of immobilization of BTS for 1, 2, 3, 4, 5 and 6 times, with the inset showing the plate viable count of BTS-MSFT4.

higher than that of free colonies with 1.09×10^8 cfu mL^{-1}, fully indicating that the immobilized BTS method greatly increased the microorganism activity in this experiment. Comprehensive analysis of the above results shows that the immobilization method of this experiment significantly improves the number and activity of microorganisms, and the biodegradable PVA adhesive can firmly fix the microorganism inoculum on the material and reduce the loss of microorganisms during the experiment, which in turn provides a feasible method for immobilization of the BTS strain owing to its low biological toxicity, high physical/chemical stability, and strong biocompatibility.

After loading the BTS strain, the surface of the BTS-MSFT4 was remodified with MTMS to achieve a surficial hydrophobic wettability for selective adsorption of oils or petroleum contaminants from water (abbreviated as BTS-MSFT4@MTMS), as shown in Figure 5. As shown in Figure 5a, the WCA was measured to be 110° after hydrophobic modification, indicating that the superhydrophilic BTS-MSFT4 changes into lipophilic BTS-MSFT4@MTMS. Moreover, the SEM image of the BTS-MSFT4@MTMS (Figure 5b) shows a smooth surface morphology, quite different from that of the BTS-MSFT, which has an apparently rough surface. Analysis from EDS (Figure 5c) shows that there is a rich distribution of the Si element, further confirming the successful surface modification. As shown in Figure S3, after modification, we counted the number of viable bacteria for BTS in BTS-MSFT4@MTMS and found that the hydrophobic modifica-

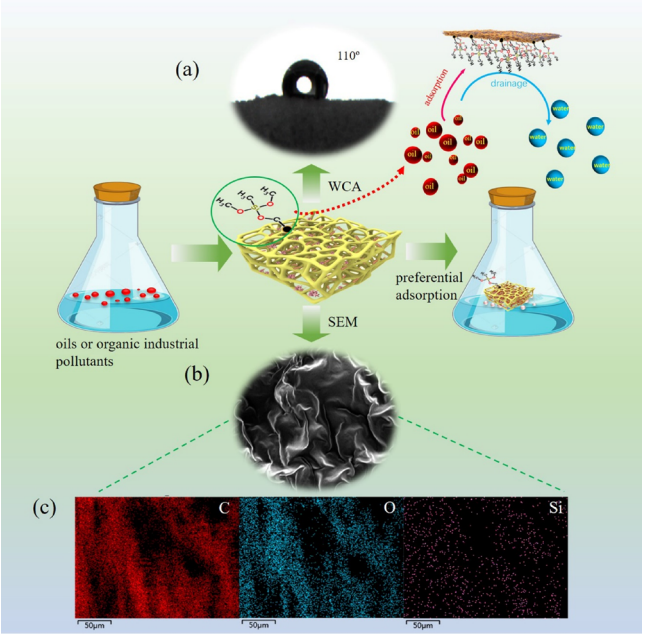

Figure 5. Schematic illustration for the selective adsorption mechanism of BTS-MSFT4@MTMS; (a) WCA of BTS-MSFT4@MTMS, (b) SEM image of BTS-MSFT4@MTMS; (c) EDS elemental image of BTS-MSFT4@MTMS showing the distribution of C, O, and Si.

https://doi.org/10.1021/acsami.1c15380
ACS Appl. Mater. Interfaces 2021, 13, 53586−53598

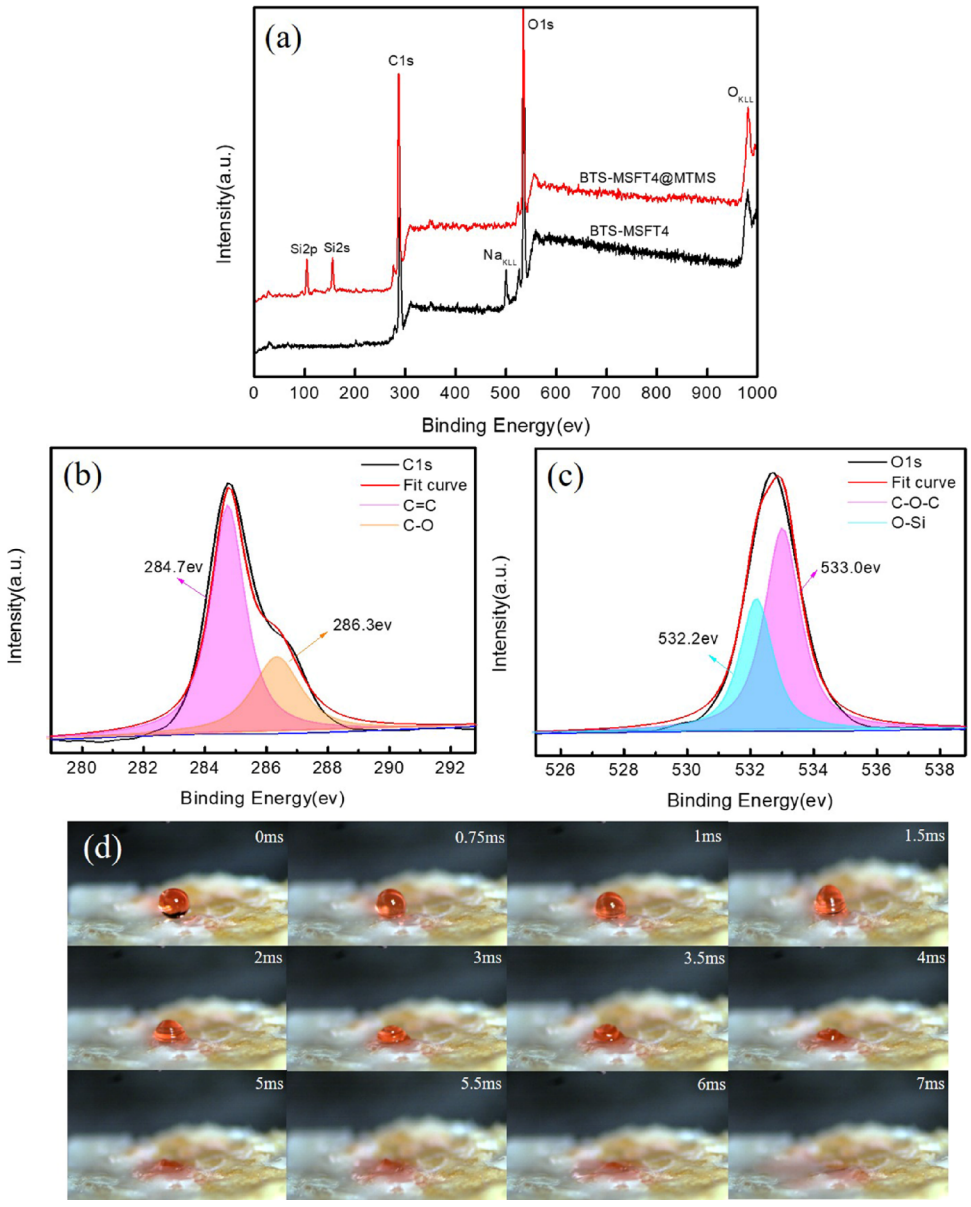

Figure 6. (a) XPS spectra of BTS-MSFT4 and BTS-MSFT4@MTMS, high-resolution XPS spectra for (b) C 1s and (c) O 1s of the BTS-MSFT4@MTMS, and (d) camera photos of the petroleum adsorption process on the surface of BTS-MSFT4@MTMS.

tion did not affect the activity of BTS, and the number of BTS was as much as that of BTS-MSFT4 when diluted 8 times.

In Figure 6a, the BTS-MSFT4 mainly contains elements C 1s and O 1s before modification, the elements Si 2p and Si 2s are added to the XPS spectra of BTS-MSFT4, indicating that the BTS-MSFT4 was successfully modified by MTMS, which is in good agreement with the result obtained in EDS measurement. The C 1s spectra of Figure 6b clearly illustrate that 284.7 and 286.3 eV belong to the peaks of C═C and C−O, respectively. Meanwhile, in the O 1s spectra (as shown in Figure 6c), 532.2 and 533.0 eV belong to the peaks of O−Si and C−O−C, respectively. From the shot images (Figure 6d), we know that the time from droplet dropping to complete immersion is only 7 ms, suggesting excellent lipophilicity, i.e., strong oil affinity, which would be beneficial to selective adsorption and biodegradation of oils or petroleum pollutants. As shown in Figure S4, the maximum load and elastic modulus of the material increase after immobilization and modification, and the maximum load and elastic modulus of the final material BTS-MSFT4@MTMS are 2992.71 N and 11.08 N mm^{-2}, respectively. The results indicate that BTS-MSFT4@MTMS has excellent mechanical strength, which is beneficial to practical application. From the mercury intrusion/extrusion curves (as shown in Figure S5), it can be seen that the curves of BTS-MSFT4 and BTS-MSFT4@MTMS are similar; when the diameter is 350−80 μm, the pore volume amount increases slowly, and when the diameter is 80−0 μm, the pore volume amount increases rapidly. Moreover, the cumulative range of their pore size is 0−50 μm. The porosities of BTS-MSFT4 and BTS-MSFT4@MTMS are 86.84 and 84.21%, respectively, indicating that BTS-MSFT4 and BTS-MSFT4@MTMS are still macroporous structures, but compared with the raw materials, the pore size and porosity are reduced. This is due to the use of PVA as an adhesive to immobilize BTS. In addition, the porosity of BTS-MSFT4 and BTS-MSFT4@MTMS is

https://doi.org/10.1021/acsami.1c15380
ACS Appl. Mater. Interfaces 2021, 13, 53586−53598

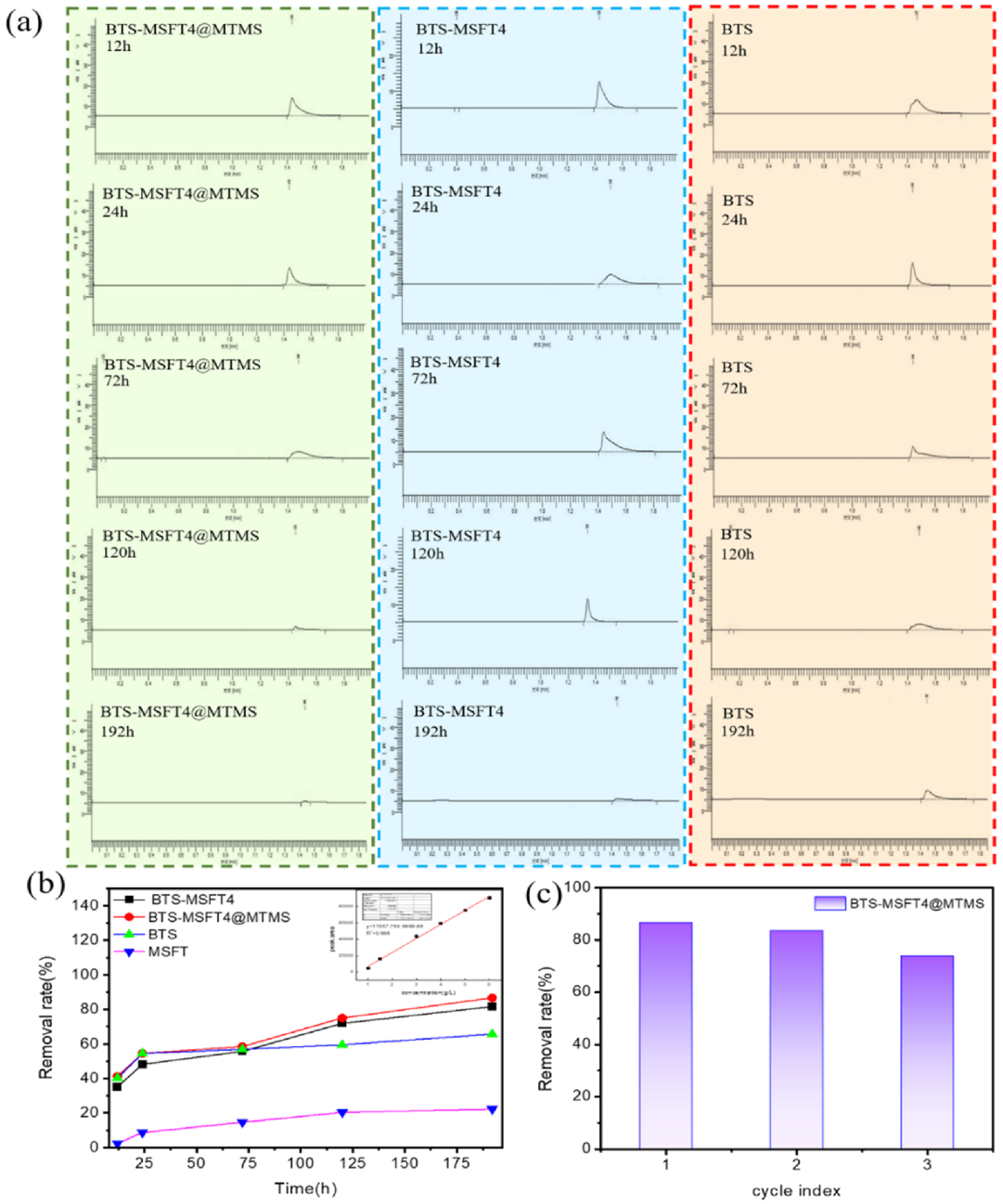

Figure 7. (a) GC originals for BTS-MSFT4@MTMS, BTS-MSFT4, and BTS. (b) The temperature was 37 °C, pH = 7, and the rotating speed of the rocking bed was 120 r min^{-1}. BTS, MSFT, BTS-MSFT4, and BTS-MSFT4@MTMS were used to remove 3% *n*-hexadecane at different times, with the inset showing the standard curve of simulated petroleum *n*-hexadecane. (c) The temperature was 37 °C, pH = 7, and the rotating speed of the rocking bed was 120 r min^{-1}. Reuse of BTS-MSFT4@MTMS to degrade the 3% *n*-hexadecane mixed liquid.

similar, which indicates that hydrophobic modification does not affect the porosity of the material.

Figure 7a and Figure S6 show the results of gas chromatography (GC). Here, the peak area refers to the content of model petroleum, which in this is case *n*-hexadecane. It can be seen that the peak area for all samples decreases with the increase in the time, implying that *n*-hexadecane can be degraded gradually with the prolonged time. It should be noted that the smallest peak area was observed for BTS-MSFT4@MTMS at 192 h compared to those of BTS-MSFT4, BTS, and MSFT, i.e., the residual amount of *n*-hexadecane is the lowest for BTS-MSFT4@MTMS, indicating the optimal degradation rate for *n*-hexadecane. After a duration of 192 h, the changes in morphology of BTS-MSFT4@MTMS were investigated by SEM. As shown in Figure S7, it still has a good porous structure, showing better stability.

The degradation activities of BTS-MSFT4 (experimental group 1), BTS-MSFT4@MTMS (experimental group 2), BTS (control group), and MSFT (blank group) on the simulated petroleum *n*-hexadecane of 3% concentration have been determined by the adsorption comparison experiment. Moreover, the degradation rate of *n*-hexadecane was calculated using formula S2. As shown in Figure 7b, the degradation rate gradually increased with the increase in degradation time for degradation for 120 h, and the degradation rates of BTS-

https://doi.org/10.1021/acsami.1c15380
ACS Appl. Mater. Interfaces 2021, 13, 53586−53598

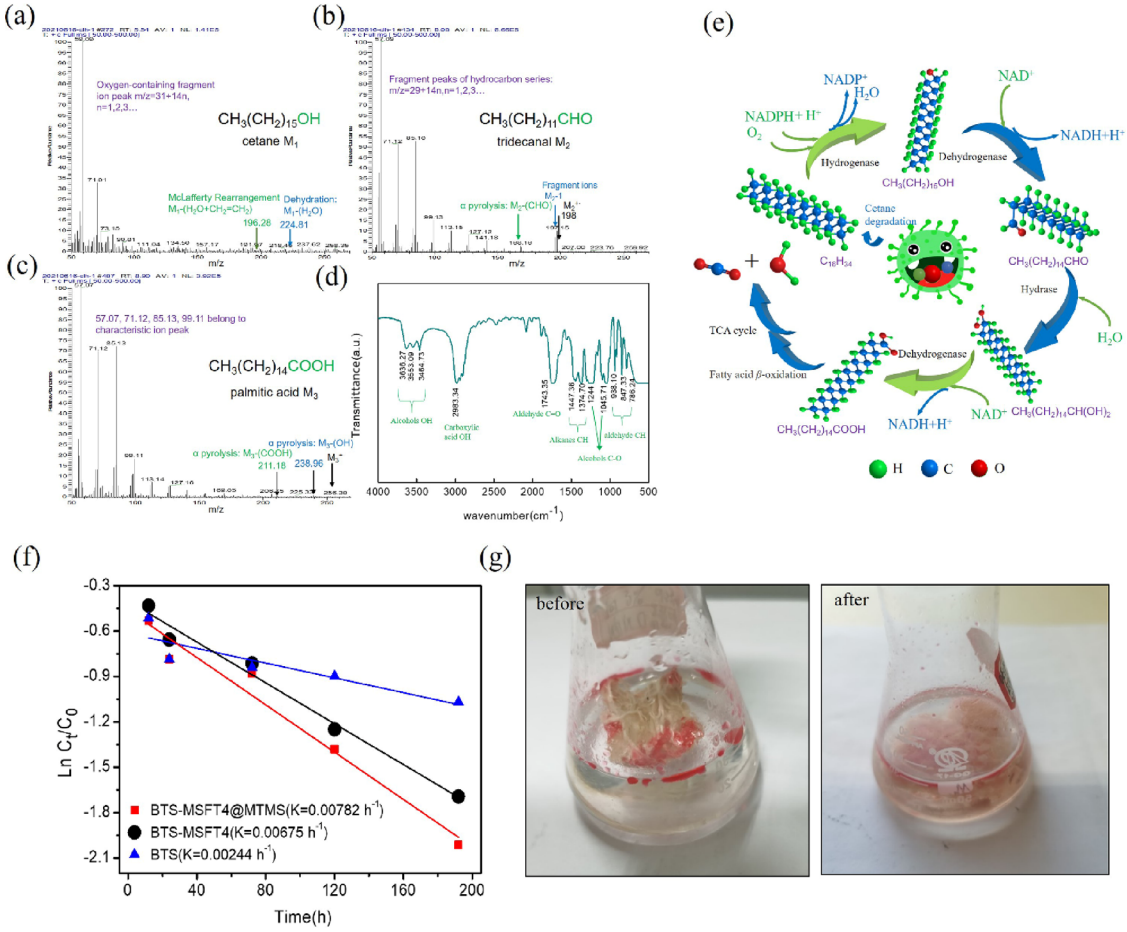

Figure 8. (a) GC−MS spectrogram of alcohol intermediates produced by degradation; (b) GC−MS spectrogram of aldehyde intermediates produced by degradation; (c) GC−MS of fatty acid intermediates produced by degradation; (d) FTIR spectra of the intermediate produced by degradation; (e) theoretical degradation mechanism diagram of *n*-hexadecane by microorganisms through terminal oxidation; (f) comparison diagram of the first-order dynamics of BTS-MSFT4@MTMS, BTS-MSFT4, and BTS when pH = 7, temperature = 37 °C, and the rotating speed of the rocking bed = 120 r min^{-1}; (g) BTS-MSFT4@MTMS rendering of degradation of *n*-hexadecane (oil red O stain).

MSFT4 and BTS-MSFT4@MTMS tended to be stable. At 192 h, the degradation rates of BTS-MSFT4@MTMS reached a maximum of 86.65% and BTS-MSFT4 reached 81.62%, while the control BTS tended to be stable after 24 h. The above results may be attributed to the fact that when the free BTS contacts with the water−oil mixture containing 3% simulated petroleum *n*-hexadecane, the bacteria quickly absorb and degrade *n*-hexadecane to obtain energy for their growth and reproduction or convert *n*-hexadecane into their own component through assimilation.[37] However, the degradation rate tended to be lower, which continued during the later stage of degradation due to a large number of dead microorganisms caused by the lack of a carbon source. The analysis of the degradation curves of the blank group showed that the material itself has adsorption activity and can effectively improve the biological effective concentration at the microenvironment of BTS-MSFT4 and BTS-MSFT4@MTMS, which leads to improving the contact rate with *n*-cetane of the simulated petroleum,[41] thus enhancing the degradation rate.

The reusability of the material is also an important property. Therefore, we have carried out three repeated experiments on BTS-MSFT4@MTMS at 37 °C, pH = 7, and 120 r min^{-1}. However, after the first degradation, we needed to dry BTS-MSFT4@MTMS and reload the BTS inoculum. This is because the microorganism has a half-life. To ensure that the microorganism has good activity, we reloaded 2 g of BTS in BTS-MSFT4@MTMS and then carried out the degradation experiment. As shown in Figure 7c, the degradation rate decreased with the increase in reuse times. This is because when BTS is loaded, the pore size of the material is reduced. With the increase in cycle times, the pore size of BTS-MSFT4@MTMS became smaller and smaller. The second reason is that in the degradation process, the material itself provides nutrition for microorganisms, so the structure is gradually broken due to degradation, resulting in poor degradability.

To verify the biodegradation mechanism of *n*-hexadecane by BTS-MSFT4@MTMS, gas chromatography−mass spectrometry (GC−MS) was used to detect the components of residues after 7 days of biodegradation of *n*-hexadecane. Figure 8a, Figure 8b, and Figure 8c show the GC−MS spectra of alcohols, aldehydes, fatty acids, and other substances produced by microorganism degradation of *n*-hexadecane, respectively. Their classification is judged by different characteristic ion peaks of different functional groups. The chemical structure was analyzed by $M^{+\cdot}$ or dehydration, characteristic ion peaks, α pyrolysis, and so on. As shown in Figure 8a, peaks around 59, 73, 83, and 111 are oxygen-containing fragment ion peaks of alcohol; the molecular ion peak of alcohols is generally weak or does not appear, with the dehydration (M-18) peak at 224.81

https://doi.org/10.1021/acsami.1c15380
ACS Appl. Mater. Interfaces 2021, 13, 53586−53598

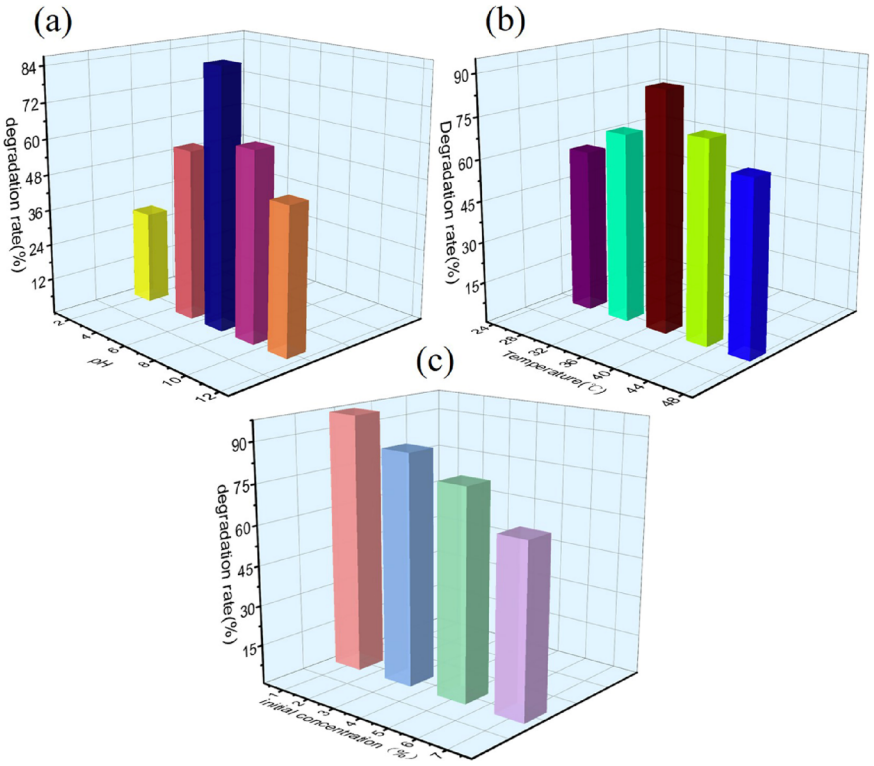

Figure 9. (a) BTS-MSFT4@MTMS degradation rate in different pH environments, (b) BTS-MSFT4@MTMS degradation rate at different temperatures, and (c) BTS-MSFT4@MTMS degradation rates at different initial concentrations of *n*-cetane.

and the McLafferty rearrangement (M-(H_2O+CH_2=CH_2)) peak at 196.28, so it can be judged as hexadecanol. Peaks near 57, 85, 99, 113, and 127 in Figure 8b are fragment peaks of the hydrocarbon series of aldehydes, and the $M^{+\cdot}$ peak at 198, the fragment ion (M-1) peak at 197.15, and the α pyrolysis(M-(CHO)) peak at 168.16 can be assigned to tridecanal. Peaks near 57, 71, and 85 in Figure 8c are characteristic ion peaks of fatty acids, the peak of $M^{+\cdot}$ is at 256.30, and the peaks of α pyrolysis (M-(COOH) and M-(OH)) are at 211.18 and 238.9, respectively, which can be attributed to palmitic acid. As shown in Figure 8d, the FTIR spectra during degradation can be observed, in which 3636.27, 3553.09, and 3464.73 are the OH stretching vibration peaks in alcohols and 2983.34 is the OH stretching vibration peak in carboxylic acids. The 1743.35 value belongs to the stretching vibration peak of C=O, 1447.36 and 1374.70 are the stretching vibration peaks of CH for alkanes, 1244 and 1045.71 are the stretching vibration peaks of C−O for alcohols, and 938.10, 847.33, and 786.24 are the stretching vibration peaks of CH in aldehydes. All the above results indicate that alcohols, aldehydes, fatty acids, and other substances are produced during the degradation of *n*-hexadecane. Also, the molecular chain is gradually shortened and finally converted into H_2O and CO_2.

Theoretically, there are three degradation ways for *n*-alkanes with a carbon number greater than 1: oxidation at the end of alkanes, oxidation at the second end, and oxidation at the two ends, which gradually produce alcohols, aldehydes, and fatty acids, then enter the TCA cycle through β oxidation, and finally produce CO_2 and H_2O. Among them, alkane terminal oxidation is the most common, as shown in Figure 8e. In our experiment, the intermediates such as hexadecanol, tridecanal, and palmitic acid produced by degradation are detected, suggesting that the degradation pattern for *n*-hexadecane in this study is well in accordance with that of the alkane terminal oxidation mechanism.

We also carried out a degradation kinetics study, and the results are shown in Figure 8f. The first-order dynamics results show that the degradation rate of BTS-MSFT4@MTMS is the fastest, and the rate constants of BTS-MSFT4@MTMS, BTS-MSFT4, and BTS are 0.00782, 0.00675, and 0.00244 h^{-1}, respectively, calculated using formula S3. The half-lives ($t_{1/2}$) of BTS-MSFT4@MTMS, BTS-MSFT4, and BTS are 88.64, 102.69, and 288.81 h, respectively, calculated using formula S4. The half-lives of the control group BTS and the experimental group BTS-MSFT4 show that the porous material BTS-MSFT4 possesses a rich pore structure, and the degradation of flora exists in its internal pores, which provides a suitable microenvironment for microorganisms to survive and avoids the influence of external adverse factors. Moreover, the nutrient elements of the material can be directly supplied to the degradation bacteria BTS for consumption, thus promoting the growth of the degradation bacteria BTS.[42] At the same time, the immobilization method in this study exhibited a greater advantage on avoiding the weak binding force compared to the traditional adsorption method, by using PVA to firmly load the bacteria BTS on the pores of the material, and then, PVA was cross-linked with Ca^{2+} to shape it, thus significantly improving the degradation efficiency of *n*-hexadecane. The selective adsorption modification of BTS-MSFT4@MTMS based on BTS-MSFT4, which can prolong the carbon chain on the surface of porous materials and reduce the interface tension, exhibits hydrophobic and lipophilic properties, while the half-life reduced to 14.05 h and the degradation rate of BTS-MSFT4 increased to 5%. Combined with the analysis of the degradation sensory diagram in Figure 8g, when the BTS-MSFT4@MTMS was added into the

https://doi.org/10.1021/acsami.1c15380
ACS Appl. Mater. Interfaces 2021, 13, 53586−53598

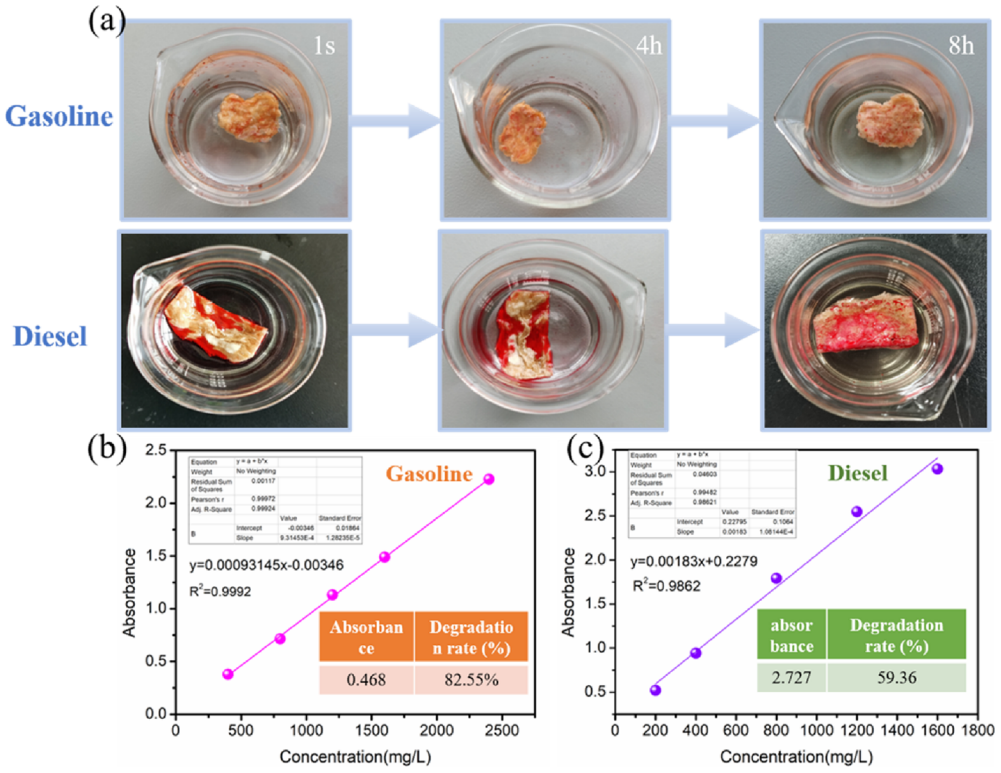

Figure 10. (a) Sensory diagram of selective adsorption of gasoline and diesel oil by BTS-MSFT4@MTMS; (b) degradation rate and standard curve of gasoline, when the degradation conditions are pH = 7, temperature = 37 °C, and the rotating speed of the rocking bed = 120 r min^{-1}; (c) degradation rate and standard curve of diesel oil, when the degradation conditions are pH = 7, temperature = 37 °C, and the rotating speed of the rocking bed = 120 r min^{-1}.

mixture of *n*-hexadecane and water, *n*-hexadecane aggregated in the center and was selectively adsorbed by the material instantly. Based on BTS-MSFT4, the contact rate between degrading bacteria and *n*-hexadecane was enhanced, and a selective permeation membrane was formed outside, which made the microorganism more firmly fixed on BTS-MSFT4@MTMS. So, the degradation rate was significantly improved.

To evaluate the tolerance of the BTS-MSFT4@MTMS in terms of the degradation of *n*-hexadecane, the effects of different factors such as pH, concentration, and temperature of the system were studied. Their effect can be seen from Figure 9a, the tolerance of BTS-MSFT4@MTMS for the environment at different pH values shows that the degradation process is suitable for neutral environments, and the possible reason is that the surface charge and the ionization degree of the immobilized materials are very easily affected by the pH value of the solution, thus affecting its functional group characteristics and surface lipophilic characteristics. The lower the pH value of the solution, the more the hydronium ions (H_3O^+) and the greater the resistance. When the pH value is too low, the hydronium ions (H_3O^+) will occupy the linking groups attached to the microorganism cell wall on the surface and pores of BTS-MSFT4@MTMS, which will produce a repulsive force to prevent *n*-hexadecane from approaching the cells.[43] However, BTS-MSFT4@MTMS has a certain tolerance in acid and alkali environments because BTS-MSFT4@MTMS is more less affected by the pH value, and BTS-MSFT4@MTMS has stronger tolerance to alkalinity than acidity. The degradation rate of *n*-hexadecane by BTS-MSFT4@MTMS at different temperatures shows that (as shown in Figure 9b) the optimum temperature for degradation is 37 °C, it shows a certain tolerance, and the degradation rate can reach more than 50% under the conditions of different temperatures of 27 °C low temperature and 28 °C high temperature. All the above results show that the material itself has the advantage of resisting the harsh external environment, and the material has strong stability by concentrating and immobilizing BTS many times and selectively adsorbing hydrophobic modification. Therefore, the degradation ability under a severe degradation environment is improved.

Under the conditions of 192 h, 37 °C, 120 r min^{-1}, and pH = 7, with the higher concentration of *n*-hexadecane, it is easier for the adsorption sites of the surface of BTS-MSFT4@MTMS to be occupied, the utilization rate of BTS-MSFT4@MTMS is higher, the adsorption rate is higher, and the amount of *n*-hexadecane adsorbed per unit quantity BTS-MSFT4@MTMS is also relatively larger.[44] Nevertheless, when the concentration of *n*-hexadecane exceeds a certain range, the saturation of the adsorption site will also increase and the empty binding points will gradually decrease. The adsorption amount will not continue to increase due to the saturation of the adsorption sites on the surface of BTS-MSFT4@MTMS, which will result in the reduction of the adsorption rate of *n*-hexadecane. Moreover, with the increasing concentration of *n*-hexadecane, the process of adsorption for *n*-hexadecane will increase the toxicity to BTS and will affect or even inhibit the growth and metabolic activities of organisms, thus inhibiting the adsorption and degradation process.[45] Therefore, as shown in Figure 9c, the initial concentration is higher, the degradation rate is lower, and the degradation rate can reach about 96.88% when the initial concentration is 1%; although the degradation rate decreases at a high concentration of 7%, it can also reach

https://doi.org/10.1021/acsami.1c15380
ACS Appl. Mater. Interfaces 2021, 13, 53586−53598

to more than 60%. The results show that BTS-MSFT4@MTMS has a good degradation effect on *n*-hexadecane, and it can also be proven that it has a high efficiency and green degradation performance on *n*-alkanes.

In order to investigate the tolerance times of BTS-MSFT4@MTMS to harsh environments, we used BTS-MSFT4@MTMS to repeatedly degrade 3% hexadecane simulated pollutants at different concentrations, different pHs, and different temperatures and tested its degradation rate. To keep the material active, before each degradation, we dried the material and added an appropriate amount of PVA and BTS. The degradation rate test results are shown in Figure S8. Under different pHs, temperatures, and initial concentrations, the degradation rate decreased with the increase in cycle times. However, when the cycle is at the third time, BTS-MSFT4@MTMS still has certain tolerance to the environment. The reason is that microbes have a half-life, and their activity gradually decreases with the increase in cycle times.

Diesel oil and gasoline are petroleum products, and their demand is increasing year by year with the development of social economy. Due to their unreasonable utilization and disposal by human beings, a large amount of diesel oil enters the groundwater system, causing serious harm to it and threatening people's health and life. So, to further prove that BTS-MSFT4@MTMS can be applied to petroleum degradation, we chose diesel oil and gasoline commonly used in petroleum products as pollutants and used BTS-MSFT4@MTMS to selectively adsorb and degrade a 3% water−oil mixture. As shown in Figure 10a, the adsorption of diesel oil and gasoline by BTS-MSFT4@MTMS can reach 99% in 8 h. On the fourth day, the degradation rates of BTS-MSFT4@MTMS to gasoline and diesel are 82.55 and 59.36%, respectively, as shown in Figure 10b and Figure 10c. Among them, the volatilization of gasoline leads to an increase in its degradation rate. This BTS-MSFT4@MTMS with selective adsorption and biodegradation has great practical application potential in environmental remediation.

4. CONCLUSIONS

In conclusion, we have demonstrated a new strategy for selective adsorption and then efficient biodegradation of petroleum pollutants by fabrication and employment of an ultralight and lipophilic microorganism-loaded biomass porous foam under mild conditions. By a simple surface modification, petroleum can be selectively absorbed into the biomass porous foam for biodegradation by the preimmobilized BTS strain. The results obtained from this study show that the degradation rate of 3% *n*-hexadecane by BTS-MSFT4@MTMS was as high as 86.65% within 8 days, which is increased by 27% compared with that of free BTS. The biodegradation mechanism of *n*-hexadecane by BTS-MSFT4@MTMS was also studied by a GC−MS spectrometer, and the results suggest an alkane terminal oxidation degradation pattern. The investigation of the effect of external environment conditions on the tolerance of BTS-MSFT4@MTMS shows that BTS-MSFT4@MTMS has a good tolerance and stability. Compared with the existing methods for removal of petroleum pollution by direct adsorption of petroleum pollution via superoleophilic porous materials or applying of a free BTS strain for biodegradation only, which suffers the drawbacks of low selectivity or poor efficiency, our method has great advantages of cost-effectiveness, scalable fabrication, and high efficiency without secondary pollution, thus showing significant potential for practical applications.

ASSOCIATED CONTENT

Supporting Information

The Supporting Information is available free of charge at https://pubs.acs.org/doi/10.1021/acsami.1c15380.

Equations related to this work, camera photos of the water adsorption process on the surface of the MSFT, group chart of living-bacteria plate counting of BTS-MSFT4, GC originals for the MSFT, and SEM images of BTS-MSFT4@MTMS after degradation for 192 h (PDF)

AUTHOR INFORMATION

Corresponding Authors

Lihua Chen − *Key Laboratory of State Ethnic Affairs Commission, College of Chemical Engineering, Northwest Minzu University, Lanzhou 730030, P. R. China;* orcid.org/0000-0002-2094-2279; Phone: +86-0931-4512929; Email: clh@xbmu.edu.cn; Fax: +86-0931-4512930

An Li − *College of Petrochemical Technology, Lanzhou University of Technology, Lanzhou 730050, P. R. China;* orcid.org/0000-0003-1982-1880; Phone: +86-931-7823125; Email: lian2010@lut.cn; Fax: +86-931-7823125

Authors

Kaihui Xu − *Key Laboratory of State Ethnic Affairs Commission, College of Chemical Engineering, Northwest Minzu University, Lanzhou 730030, P. R. China*

Yuhan Zhang − *Key Laboratory of State Ethnic Affairs Commission, College of Chemical Engineering, Northwest Minzu University, Lanzhou 730030, P. R. China*

Qimeige Hasi − *Key Laboratory of State Ethnic Affairs Commission, College of Chemical Engineering, Northwest Minzu University, Lanzhou 730030, P. R. China*

Xiaofang Luo − *Center of Experiment, Northwest Minzu University, Lanzhou 730030, P. R. China*

Juanjuan Xu − *Key Laboratory of State Ethnic Affairs Commission, College of Chemical Engineering, Northwest Minzu University, Lanzhou 730030, P. R. China*

Complete contact information is available at: https://pubs.acs.org/10.1021/acsami.1c15380

Notes

The authors declare no competing financial interest.

ACKNOWLEDGMENTS

This work is supported by the National Natural Science Foundation of China (Grant No. 21966028), the 2021 Key Talent Project of Gansu, Science and Technology Project of Gansu (Grant No. 21YF5GA062, 21JR1RA204), Science and Technology Project of Lanzhou (Grant No. 2021-1-138), the Fundamental Research Funds for the Central Universities (Grant No. 31920210139, 31920210062, and 31920210136).

REFERENCES

(1) Margesin, R.; Moertelmaier, C.; Mair, J. Low-temperature biodegradation of petroleum hydrocarbons (n-alkanes, phenol, anthracene, pyrene) by four actinobacterial strains. *Int. Biodeterior. Biodegrad.* **2013**, *84*, 185−191.

(2) Tiwari, B.; Manickam, N.; Kumari, S.; Tiwari, A. Biodegradation and dissolution of polyaromatic hydrocarbons by Stenotrophomonas sp. *Bioresour. Technol.* **2016**, *216*, 1102−1105.
(3) Wang, X.; Li, M.; Shen, Y.; Yang, Y.; Feng, H.; Li, J. Facile preparation of loess-coated membranes for multifunctional surfactant-stabilized oil-in-water emulsion separation. *Green Chem.* **2019**, *21*, 3190−3199.
(4) Carpenter, A. Oil pollution in the north sea: the impact of governance measures on oil pollution over several decades. *Hydrobiologia* **2019**, *845*, 109−127.
(5) Ingrid, L.; Lounes-Hadj Sahraoui, A.; Frederic, L.; Yolande, D.; Joel, F. Arbuscular mycorrhizal wheat inoculation promotes alkane and polycyclic aromatic hydrocarbon biodegradation: Microcosm experiment on aged-contaminated soil. *Environ. Pollut.* **2016**, *213*, 549−560.
(6) O'Brien, P. L.; DeSutter, T. M.; Casey, F. X. M.; Wick, A. F.; Khan, E. Evaluation of soil function following remediation of petroleum hydrocarbons—a review of current remediation techniques. *Curr. Pollut. Rep.* **2017**, *3*, 192−205.
(7) Martin, B. C.; George, S. J.; Price, C. A.; Ryan, M. H.; Tibbett, M. The role of root exuded low molecular weight organic anions in facilitating petroleum hydrocarbon degradation: current knowledge and future directions. *Sci. Total Environ.* **2014**, *472*, 642−653.
(8) Vogt, C.; Kleinsteuber, S.; Richnow, H. H. Anaerobic benzene degradation by bacteria. *Microb. Biotechnol.* **2011**, *4*, 710−724.
(9) Wei, Y.; Han, J.; Wang, Y.; Wang, H.; Sun, Y.; Yan, B. Effects of oil pollution on water movement in soils with different textures. *Water Air Soil Poll.* **2020**, *231*, 1−12.
(10) Ramadass, K.; Kuppusamy, S.; Venkateswarlu, K.; Naidu, R.; Megharaj, M. Unresolved complex mixtures of petroleum hydrocarbons in the environment: An overview of ecological effects and remediation approaches. *Crit. Rev. Env. Sci. Tec.* **2020**, *21*, 1−23.
(11) Meng, L.; Bao, M.; Sun, P. Construction of long-chain alkane degrading bacteria and its application in bioremediation of crude oil pollution. *Int. J. Biol. Macromol.* **2018**, *119*, 524−532.
(12) Tursi, A.; De Vietro, N.; Beneduci, A.; Milella, A.; Chidichimo, F.; Fracassi, F.; Chidichimo, G. Low pressure plasma functionalized cellulose fiber for the remediation of petroleum hydrocarbons polluted water. *J. Hazard. Mater.* **2019**, *373*, 773−782.
(13) Zhang, B.; Guo, Y.; Huo, J.; Xie, H.; Xu, C.; Liang, S. Combining chemical oxidation and bioremediation for petroleum polluted soil remediation by BC-nZVI activated persulfate. *Chem. Eng. J.* **2020**, *382*, 123055.
(14) Zhang, C.; Zhang, Y.; Xiao, X.; Liu, G.; Xu, Z.; Wang, B.; Yu, C.; Ras, R. H. A.; Jiang, L. Efficient separation of immiscible oil/water mixtures using a perforated lotus leaf. *Green Chem.* **2019**, *21*, 6579−6584.
(15) Li, A.; Sun, H.-X.; Tan, D.-Z.; Fan, W.-J.; Wen, S.-H.; Qing, X.-J.; Li, G.-X.; Li, S.-Y.; Deng, W.-Q. Superhydrophobic conjugated microporous polymers for separation and adsorption. *Energy Environ. Sci.* **2011**, *4*, 2062−2065.
(16) Liu, X.; Ge, L.; Li, W.; Wang, X.; Li, F. Layered double hydroxide functionalized textile for effective oil/water separation and selective oil adsorption. *ACS Appl. Mater. Inter.* **2015**, *7*, 791−800.
(17) Yoo, J.; Jeon, P.; Tsang, D. C. W.; Kwon, E. E.; Baek, K. Ferric-enhanced chemical remediation of dredged marine sediment contaminated by metals and petroleum hydrocarbons. *Environ. Pollut.* **2018**, *243*, 87−93.
(18) Kang, L.; Wang, B.; Zeng, J.; Cheng, Z.; Li, J.; Xu, J.; Gao, W.; Chen, K. Degradable dual superlyophobic lignocellulosic fibers for high-efficiency oil/water separation. *Green Chem.* **2020**, *22*, 504−512.
(19) Li, J.; Li, D.; Yang, Y.; Li, J.; Zha, F.; Lei, Z. A prewetting induced underwater superoleophobic or underoil (super) hydrophobic waste potato residue-coated mesh for selective efficient oil/water separation. *Green Chem.* **2016**, *18*, 541−549.
(20) Rahmani, Z.; Rashidi, A. M.; Kazemi, A.; Samadi, M. T.; Rahmani, A. R. N-doped reduced graphene oxide aerogel for the selective adsorption of oil pollutants from water: Isotherm and kinetic study. *J. Ind. Eng. Chem.* **2018**, *61*, 416−426.
(21) Sun, H.; Li, A.; Zhu, Z.; Liang, W.; Zhao, X.; La, P.; Deng, W. Superhydrophobic activated carbon-coated sponges for separation and absorption. *ChemSusChem* **2013**, *6*, 1057−1062.
(22) Zhang, B.; Yu, S.; Zhu, Y.; Shen, Y.; Gao, X.; Shi, W.; Hwa Tay, J. Adsorption mechanisms of crude oil onto polytetrafluoroethylene membrane: Kinetics and isotherm, and strategies for adsorption fouling control. *Sep. Purif. Technol.* **2020**, *235*, 116212.
(23) Li, Z.; Wang, B.; Qin, X.; Wang, Y.; Liu, C.; Shao, Q.; Wang, N.; Zhang, J.; Wang, Z.; Shen, C.; Guo, Z. Superhydrophobic/superoleophilic polycarbonate/carbon nanotubes porous monolith for selective oil adsorption from water. *ACS Sustainable Chem. Eng.* **2018**, *6*, 13747−13755.
(24) Sun, H.; Li, A.; Qin, X.; Zhu, Z.; Liang, W.; An, J.; La, P.; Deng, W. Three-dimensional superwetting mesh film based on graphene assembly for liquid transportation and selective absorption. *ChemSusChem* **2013**, *6*, 2377−2381.
(25) Xue, J.; Zhu, L.; Zhu, X.; Li, H.; Ma, C.; Yu, S.; Sun, D.; Xia, F.; Xue, Q. Tetradecylamine-MXene functionalized melamine sponge for effective oil/water separation and selective oil adsorption. *Sep. Purif. Technol.* **2021**, *259*, 118106.
(26) Varjani, S. J. Microbial degradation of petroleum hydrocarbons. *Bioresour. Technol.* **2017**, *223*, 277−286.
(27) Varjani, S. J.; Upasani, V. N. Biodegradation of petroleum hydrocarbons by oleophilic strain of pseudomonas aeruginosa NCIM 5514. *Bioresour. Technol.* **2016**, *222*, 195−201.
(28) Wang, Z.-Y.; Xu, Y.; Wang, H.-Y.; Zhao, J.; Gao, D.-M.; Li, F.-M.; Xing, B. Biodegradation of crude oil in contaminated soils by free and immobilized microorganisms. *Pedosphere* **2012**, *22*, 717−725.
(29) Zhang, C.; Li, J.; Wu, X.; Long, Y.; An, H.; Pan, X.; Li, M.; Dong, F.; Zheng, Y. Rapid degradation of dimethomorph in polluted water and soil by Bacillus cereus WL08 immobilized on bamboo charcoal-sodium alginate. *J. Hazard. Mater.* **2020**, *398*, 122806.
(30) Bouabidi, Z. B.; El-Naas, M. H.; Zhang, Z. Immobilization of microbial cells for the biotreatment of wastewater: A review. *Environ. Chem. Lett.* **2018**, *17*, 241−257.
(31) Gao, Y.; Wang, X.; Li, J.; Lee, C. T.; Ong, P. Y.; Zhang, Z.; Li, C. Effect of aquaculture salinity on nitrification and microbial community in moving bed bioreactors with immobilized microbial granules. *Bioresour. Technol.* **2020**, *297*, 122427.
(32) Eroglu, E.; Agarwal, V.; Bradshaw, M.; Chen, X.; Smith, S. M.; Raston, C. L.; Swaminathan Iyer, K. Nitrate removal from liquid effluents using microalgae immobilized on chitosan nanofiber mats. *Green Chem.* **2012**, *14*, 2682−2685.
(33) Basak, B.; Jeon, B.-H.; Kurade, M. B.; Saratale, G. D.; Bhunia, B.; Chatterjee, P. K.; Dey, A. Biodegradation of high concentration phenol using sugarcane bagasse immobilized Candida tropicalis PHB5 in a packed-bed column reactor. *Ecotox. Environ. Safe.* **2019**, *180*, 317−325.
(34) Duan, L.; Wang, H.; Sun, Y.; Xie, X. Biodegradation of phenol from wastewater by microorganism immobilized in bentonite and carboxymethyl cellulose gel. *Chem. Eng. Commun.* **2015**, *203*, 948−956.
(35) Giese, E. C.; Silva, D. D. V.; Costa, A. F. M.; Almeida, S. G. C.; Dussan, K. J. Immobilized microbial nanoparticles for biosorption. *Crit. Rev. Biotechnol.* **2020**, *40*, 653−666.
(36) Liu, X.; Guan, Y.; Shen, R.; Liu, H. Immobilization of lipase onto micron-size magnetic beads. *J. Chromatogr., B* **2005**, *822*, 91−97.
(37) Chen, L.; Lei, Z.; Luo, X.; Wang, D.; Li, L.; Li, A. Biological degradation and transformation characteristics of total petroleum hydrocarbons by oil degradation bacteria adsorbed on modified straw. *ACS Omega* **2019**, *4*, 10921−10928.
(38) Datta, S.; Veena, R.; Samuel, M. S.; Selvarajan, E. Immobilization of laccases and applications for the detection and remediation of pollutants: a review. *Environ. Chem. Lett.* **2020**, *19*, 521−538.
(39) Zhang, B.; Zhang, L.; Zhang, X. Bioremediation of petroleum hydrocarbon-contaminated soil by petroleum-degrading bacteria immobilized on biochar. *RSC Adv.* **2019**, *9*, 35304−35311.

https://doi.org/10.1021/acsami.1c15380
ACS Appl. Mater. Interfaces 2021, 13, 53586−53598

(40) Chen, L.; Zhao, S.; Yang, Y.; Li, L.; Wang, D. Study on degradation of oily wastewater by immobilized microorganisms with biodegradable polyacrylamide and sodium alginate mixture. *ACS Omega* **2019**, *4*, 15149−15157.
(41) Meckenstock, R. U.; Boll, M.; Mouttaki, H.; Koelschbach, J. S.; Cunha Tarouco, P.; Weyrauch, P.; Dong, X.; Himmelberg, A. M. Anaerobic degradation of benzene and polycyclic aromatic hydrocarbons. *J. Mol. Microbiol. Biotechnol.* **2016**, *26*, 92−118.
(42) Li, S.; Yang, M.; Wang, H.; Zhao, Y. Dynamic characteristics of immobilized microorganisms for remediation of nitrogen-contaminated groundwater and high-throughput sequencing analysis of the microbial community. *Environ. Pollut.* **2020**, *267*, 114875.
(43) Kureel, M. K.; Geed, S. R.; Giri, B. S.; Rai, B. N.; Singh, R. S. Biodegradation and kinetic study of benzene in bioreactor packed with PUF and alginate beads and immobilized with Bacillus sp. M3. *Bioresour. Technol.* **2017**, *242*, 92−100.
(44) Leong, Y. K.; Chang, J. S. Bioremediation of heavy metals using microalgae: Recent advances and mechanisms. *Bioresour. Technol.* **2020**, *303*, 122886.
(45) Boschi, C.; Maldonado, H.; Ly, M.; Guibal, E. Cd(II) biosorption using Lessonia kelps. *J. Colloid. Interf. Sci.* **2011**, *357*, 487−496.

https://doi.org/10.1021/acsami.1c15380
ACS Appl. Mater. Interfaces 2021, 13, 53586−53598